Electronic Supplementary Material (ESI) for Dalton Transactions.

ELECTRONIC SUPPORTING INFORMATION

Switching On Single-Molecule Magnet (SMM) Properties of Homoleptic Sandwich Tris(pyrazolyl)borate Dysprosium (III) Cations via Intermolecular Dipolar Coupling

Dimitris I. Alexandropoulos, Kuduva R. Vignesh, Haomiao Xie, and Kim R. Dunbar*

Department of Chemistry, Texas A&M University, College Station, Texas 77842-3012, United States.

Table of Contents

Single crystal X-ray crystallography

Table S1. Crystal data and structural refinement parameters for compounds **1-2**.

Complex	**1**·CH_2Cl_2	**2**	**3**
Empirical formula	$C_{46}H_{68}B_3Cl_5Dy_2N_{18}$	$C_{19}H_{34}BCl_3DyN_7$	$C_{30}H_{44}B_2DyIN_{12}$
Formula weight	1407.86	640.19	883.79
Temperature/K	110.0	110.0	100.42
Crystal system	monoclinic	monoclinic	monoclinic
Space group	$P2_1/n$	$P2_1/n$	C2/m
a/Å	10.2885(5)	9.499(3)	16.4584(11)
b/Å	36.2677(19)	31.346(8)	12.8987(8)
c/Å	16.0699(9)	10.016(3)	8.4033(6)
α/°	90	90	90
β/°	92.5040(16)	118.040(8)	91.810(3)
γ/°	90	90	90
Volume/Å^3	5990.6(5)	2632.2(13)	1783.1(2)
Z	4	4	2
ρ_{calc}g/cm^3	1.561	1.615	1.646
μ/mm^{-1}	2.747	3.163	3.001
F(000)	2808.0	1276.0	874.0
Crystal size/mm^3	0.2 × 0.19 × 0.06	0.4 × 0.2 × 0.1	0.21 × 0.13 × 0.05
Radiation	MoKα (λ = 0.71073)	MoKα (λ = 0.71073)	MoKα (λ = 0.71073)
2Θ range for data collection/°	4.118 to 51.58	4.788 to 51.606	4.85 to 51.484
Index ranges	-12 ≤ h ≤ 12 -44 ≤ k ≤ 44 -19 ≤ l ≤ 19	-11 ≤ h ≤ 11 -38 ≤ k ≤ 38 -12 ≤ l ≤ 12	-20 ≤ h ≤ 20 -15 ≤ k ≤ 15 -10 ≤ l ≤ 10
Reflections collected	195830	108352	33794
Independent reflections	11476 R_{int} = 0.0483 R_{sigma} = 0.0208	5062 R_{int} = 0.0310 R_{sigma} = 0.0106	1791 R_{int} = 0.0635 R_{sigma} = 0.0231
Data/restraints/ parameters	11476 / 0 / 685	5062 / 0 / 290	1791 / 0 / 124
Goodness-of-fit on F^2	1.099	1.167	1.109
Final R^{a,b} indexes [I>=2σ (I)]	R_1 =0.0244 wR_2 = 0.0438	R_1 = 0.0237 wR_2 = 0.0527	R_1 = 0.0253 wR_2 = 0.0458
Final R^{a,b} indexes [all data]	R_1 = 0.0326 wR_2 = 0.0459	R_1 = 0.0270 wR_2 = 0.0542	R_1 = 0.0300 wR_2 = 0.0473
Largest diff. peak /hole / e Å^{-3}	0.77 / -0.69	1.04 / -1.50	0.56 / -0.77

$^a R_1 = \Sigma(||F_o| - |F_c||)/\Sigma|F_o|$. $^b wR_2 = [\Sigma[w(F_o^2 - F_c^2)^2]/\Sigma[w(F_o^2)^2]]^{1/2}$, $w = 1/[\sigma^2(F_o^2) + (ap)^2 + bp]$, where $p = [\max(F_o^2, 0) + 2F_c^2]/3$.

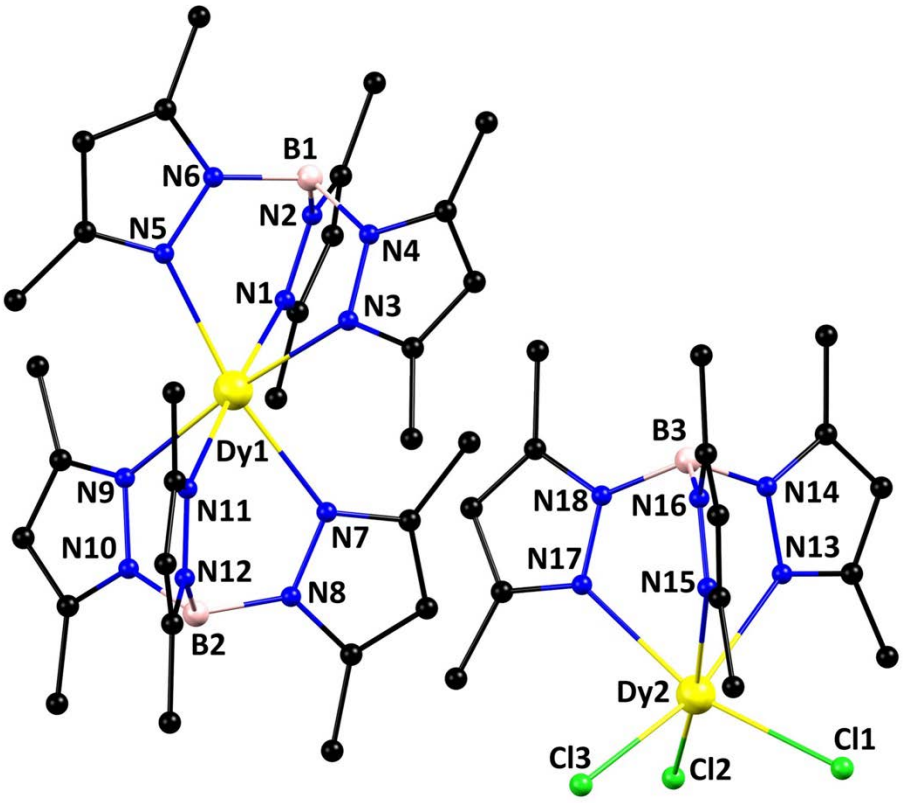

Figure S1. Molecular structure of **1**. Colors: Dy, yellow; N, blue; B, pink; Cl, green, C, black. H atoms are omitted for the sake of clarity.

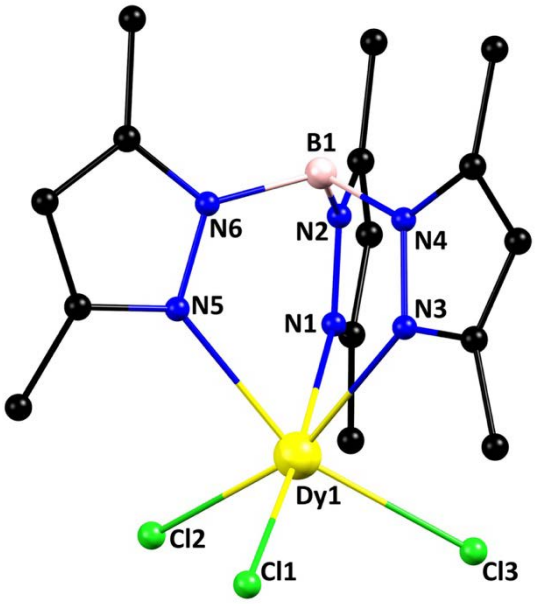

Figure S2. Labeled representation of anion **2**. Color scheme: Dy, yellow; N, blue; B, pink; Cl, green, C, black. H atoms are omitted for the sake of clarity.

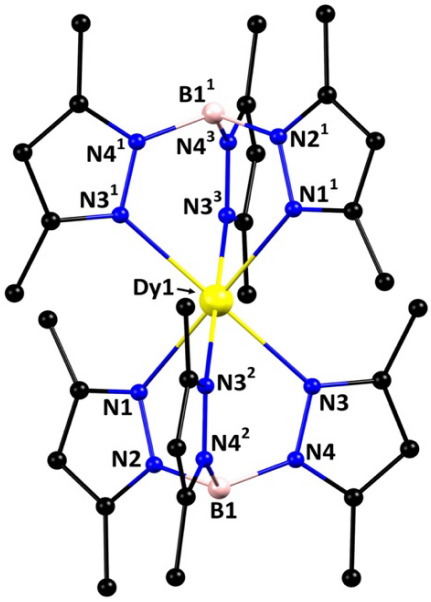

Figure S3. Labeled representation of cation **3**. Color scheme: Dy, yellow; N, blue; B, pink; Cl, green, C, black. H atoms are omitted for the sake of clarity. [1]1-X, 1-Y, 1-Z; [2]1-X, 1+Y, 1-Z; [3]1+X, 1-Y, 1+Z

Table S2. Selected bond distances and angles for compounds **1-3**.

Compound **1**			
Bond Distances (Å)			
Dy1-N1	2.383(2)	Dy2-Cl1	2.5917(7)
Dy1-N3	2.367(2)	Dy2-Cl2	2.5989(7)
Dy1-N5	2.373(2)	Dy2-Cl3	2.5869(7)
Dy1-N7	2.383(2)	Dy2-N13	2.467(2)
Dy1-N9	2.375(2)	Dy2-N15	2.445(2)
Dy1-N11	2.366(2)	Dy2-N17	2.439(2)
Bond Angles (˚)			
N3-Dy1-N1	83.68(8)	Cl1-Dy2-Cl2	99.38(3)
N3-Dy1-N5	79.81(8)	Cl3-Dy2-Cl1	100.93(2)
N3-Dy1-N7	91.59(8)	Cl3-Dy2-Cl2	96.31(2)
N3-Dy1-N9	172.60(8)	N13-Dy2-Cl1	89.57(6)
N5-Dy1-N1	79.02(8)	N13-Dy2-Cl2	93.67(6)
N5-Dy1-N7	169.63(8)	N13-Dy2-Cl3	164.12(5)
N5-Dy1-N9	106.38(8)	N15-Dy2-Cl1	89.94(6)
N7-Dy1-N1	94.38(8)	N15-Dy2-Cl2	167.30(5)
N9-Dy1-N1	101.32(8)	N15-Dy2-Cl3	90.33(6)
N9-Dy1-N7	82.64(8)	N15-Dy2-N13	77.68(8)
N11-Dy1-N1	175.85(8)	N17-Dy2-Cl1	162.20(6)
N11-Dy1-N3	97.24(8)	N17-Dy2-Cl2	93.87(6)
N11-Dy1-N5	105.12(8)	N17-Dy2-Cl3	89.30(6)
N11-Dy1-N7	81.56(8)	N17-Dy2-N13	77.70(7)
N11-Dy1-N9	77.39(8)	N17-Dy2-N15	75.34(7)
Bond Distances (Å)			
Dy1-Cl1	2.5916(10)	Dy1-N5	2.440(2)
Dy1-Cl2	2.5979(11)	Dy1-N1	2.429(2)

Dy1-Cl3	2.5740(12)	Dy1-N3	2.422(3)
Bond Angles (˚)			
Cl1-Dy1-Cl2	92.64(3)	N1-Dy1-Cl3	88.61(6)
Cl3-Dy1-Cl1	96.05(4)	N1-Dy1-N5	77.73(8)
Cl3-Dy1-Cl2	105.48(5)	N3-Dy1-Cl1	99.06(6)
N5-Dy1-Cl1	97.38(6)	N3-Dy1-Cl2	161.17(6)
N5-Dy1-Cl2	90.52(7)	N3-Dy1-Cl3	88.00(7)
N5-Dy1-Cl3	158.57(7)	N3-Dy1-N5	73.45(8)
N1-Dy1-Cl1	175.11(6)	N3-Dy1-N1	79.57(8)
N1-Dy1-Cl2	87.53(6)		
Compound **3**			
Bond Distances (Å)			
Dy1-N1[1]	2.430(3)	Dy1-N3[1]	2.376(2)
Dy1-N1	2.430(3)	Dy1-N3[2]	2.376(2)
Dy1-N3	2.376(2)	Dy1-N3[3]	2.376(2)
Bond Angles (˚)			
N1-Dy1-N1[1]	180.00(7)	N3[1]-Dy1-N1	99.56(8)
N3[2]-Dy1-N1[1]	80.44(8)	N3-Dy1-N3[2]	102.27(12)
N3[3]-Dy1-N1[1]	99.56(8)	N3[1]-Dy1-N3[2]	77.73(12)
N3-Dy1-N1	80.44(8)	N3[1]-Dy1-N3[3]	102.27(12)
N3[2]-Dy1-N1	99.56(8)	N3-Dy1-N3[1]	180.0
N3-Dy1-N1[1]	99.56(8)	N3[3]-Dy1-N3[2]	180.00(9)
N3[1]-Dy1-N1[1]	80.44(8)	N3-Dy1-N3[3]	77.73(12)
N3[3]-Dy1-N1	80.44(8)		

[1]1-X, 1-Y, 1-Z; [2]1-X, 1+Y, 1-Z; [3]1+X, 1-Y, 1+Z

Table S3. Shape measures of the six-coordinate Dy coordination polyhedra in **1-3**.

	Complex **1**		Complex **2**	Complex **3**
Polyhedron[a]	Dy1	Dy2	Dy1	Dy1
HP-6	30.33	32.44	31.80	29.51
PPY-6	25.72	28.07	26.45	28.81
OC-6	**1.55**	**1.25**	**1.70**	**1.57**
TPR-6	14.83	16.57	14.17	14.50
JPPY-6	28.73	32.78	29.58	31.67

[a] Abbreviations: HP-6, hexagon; PPY-6, pentagonal pyramid; OC-6, octahedron; TPR-6, trigonal prism; JPPY-6, Johnson pentagonal pyramid J2. The values in boldface indicate the closest polyhedron according to the Continuous Shape Measures.

Magnetism

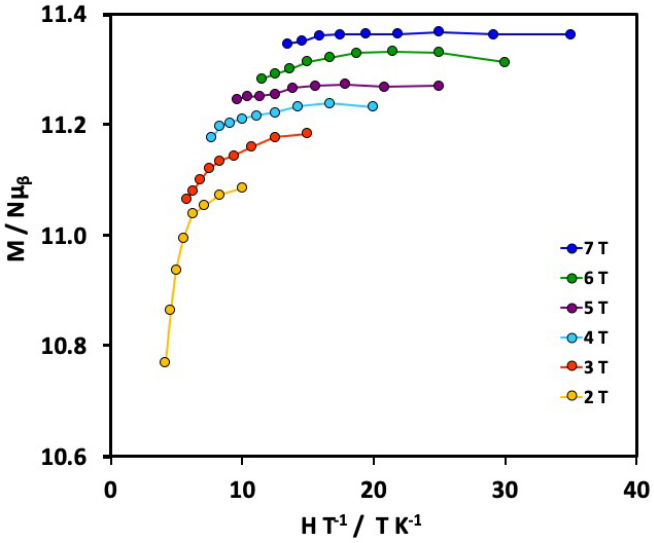

Figure S4. Plot of reduced magnetization data ($M/N\mu_B$) vs. HT^{-1} for compound **1** at applied fields of 2–7 T and in the 2–5 K temperature range. Solid lines are guides for the eye.

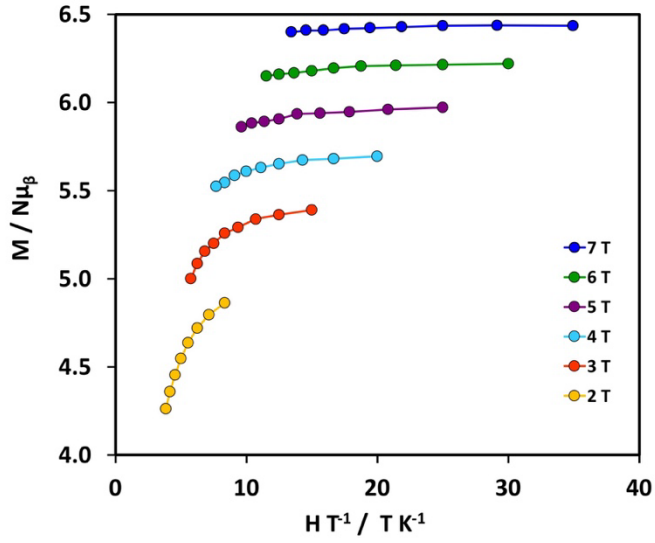

Figure S5. Plot of reduced magnetization data ($M/N\mu_B$) vs. HT^{-1} for compound **2** at applied fields of 2–7 T and in the 2–5 K temperature range. Solid lines are guides for the eye.

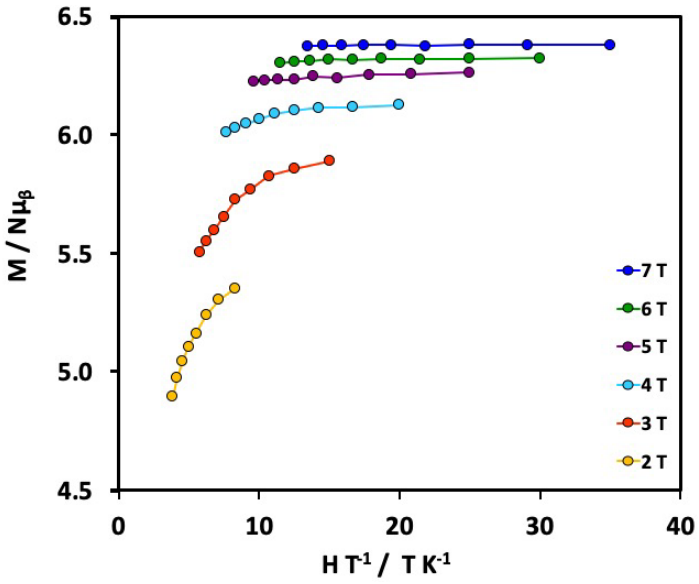

Figure S6. Plot of reduced magnetization data ($M/N\mu_B$) vs. HT^{-1} for compound **3** at applied fields of 2–7 T and in the 2–5 K temperature range. Solid lines are guides for the eye.

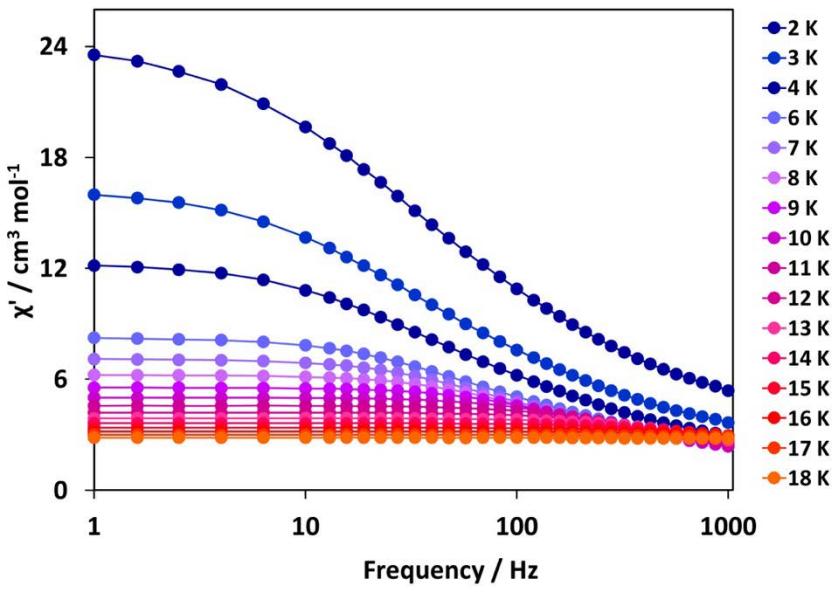

Figure S7. In-phase (χ′) component of the magnetic susceptibility vs. frequency data, under a zero applied *dc* field, for complex **1**. Solid lines are guides for the eye.

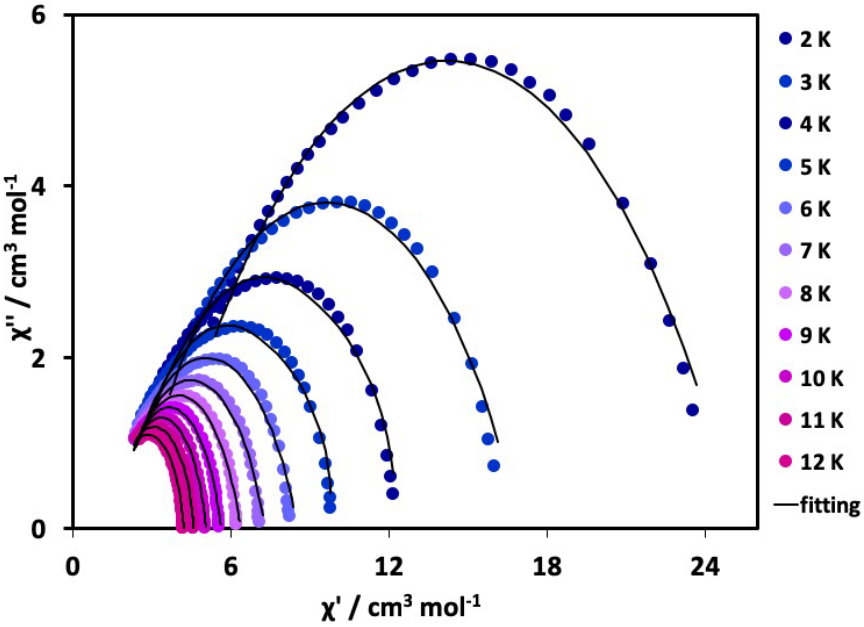

Figure S8. Cole-Cole plot for **1** obtained using the ac susceptibility data in a zero applied *dc* field. The solid lines correspond to the best fit obtained with a generalized Debye model.

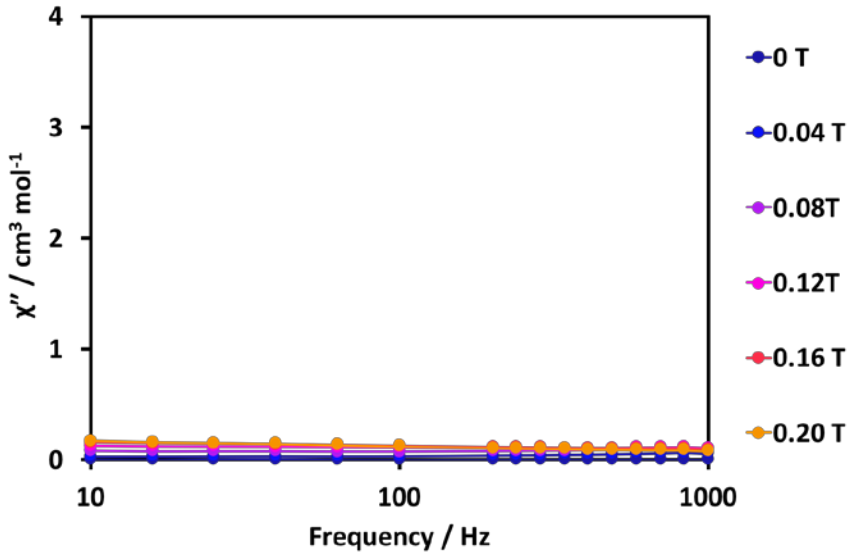

Figure S9. Out-of-phase susceptibility data for **2** in various applied DC fields at 1.8 K. Solid lines are guides for the eye.

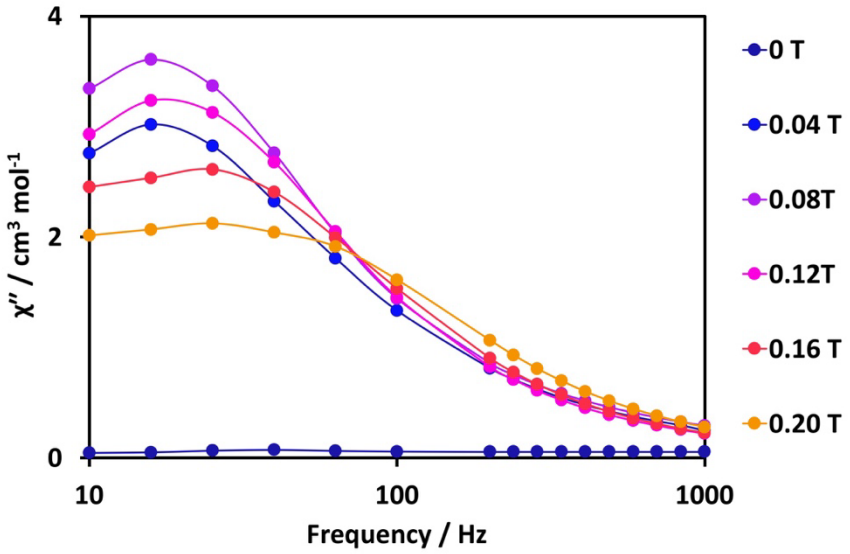

Figure S10. Out-of-phase susceptibility data for **3** in various applied DC fields at 1.8 K. Solid lines are guides for the eye.

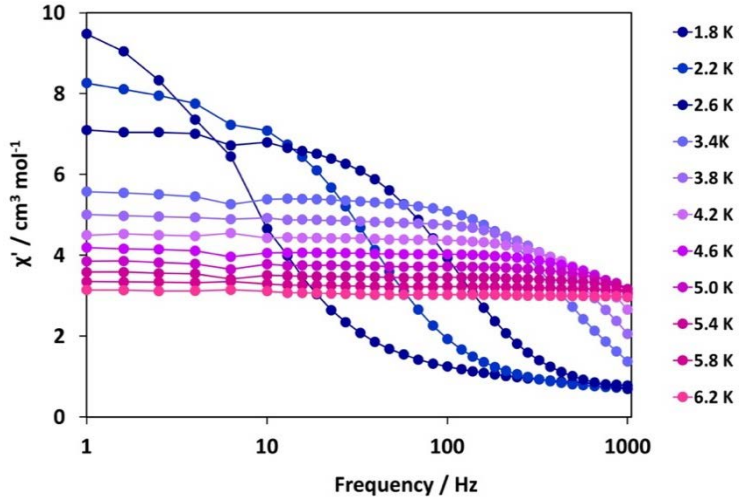

Figure S11. In-phase (χ′) component of the magnetic susceptibility vs. frequency data, under a 0.08 T applied *dc* field, for complex **3**. Solid lines are guides for the eye.

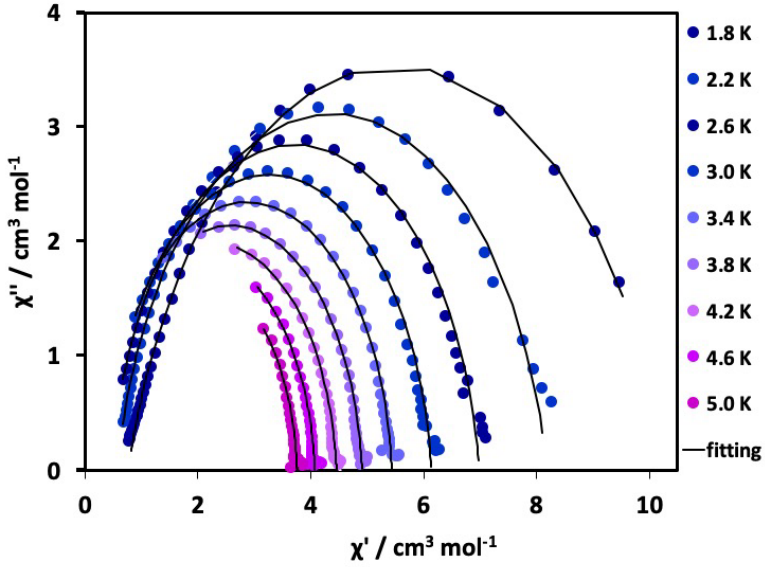

Figure S12. Cole-Cole plot for **3** obtained using the ac susceptibility data in a 0.08 T applied *dc* field. The solid lines correspond to the best fit obtained with a generalized Debye model.

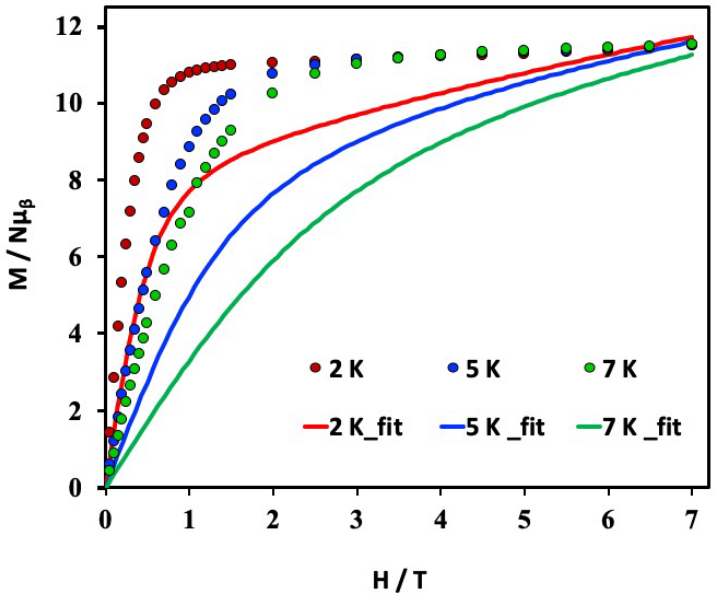

Figure S13. M vs. H plot for **1** at different low temperatures and magnetic fields. Solid lines are fittings of the experimental data.

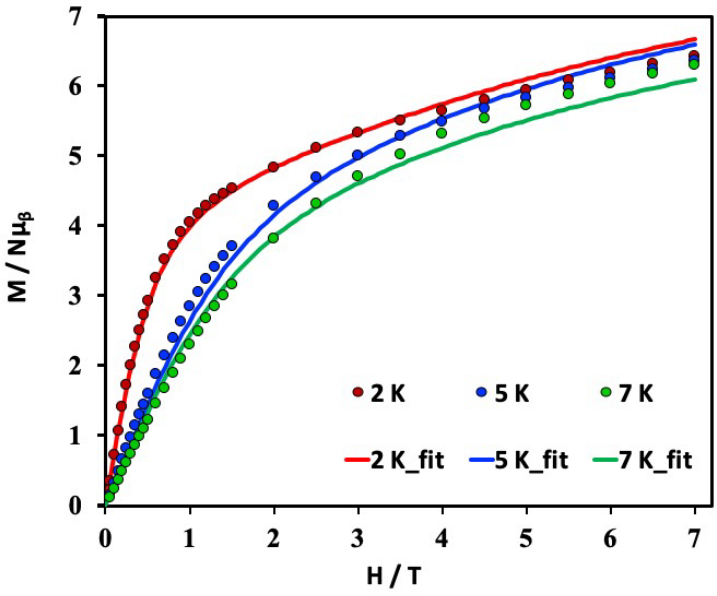

Figure S14. M vs. H plot for **2** at different low temperatures and magnetic fields. Solid lines are fittings of the experimental data.

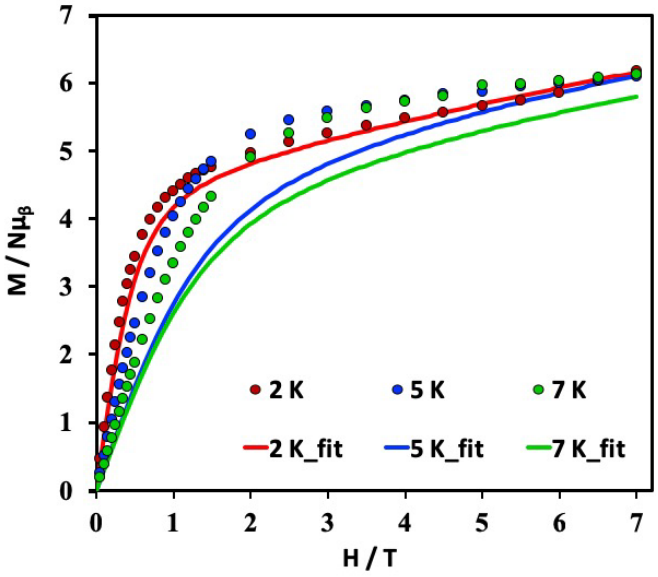

Figure S15. M vs. H plot for **3** at different low temperatures and magnetic fields. Solid lines are fittings of the experimental data.

Table S4. Cole-Cole fit values for **1**.

T (K)	ChiS	ChiT	Tau	Alpha	Residual
2	3.25E+00	2.52E+01	3.74E-03	4.12E-01	7.22E-01
3	2.27E+00	1.70E+01	3.32E-03	3.92E-01	6.56E-01
4	1.80E+00	1.28E+01	2.59E-03	3.77E-01	5.94E-01
5	1.60E+00	1.03E+01	1.97E-03	3.62E-01	5.46E-01
6	1.60E+00	8.55E+00	1.53E-03	3.35E-01	4.68E-01
7	1.66E+00	7.30E+00	1.19E-03	2.96E-01	3.51E-01
8	1.69E+00	6.36E+00	8.98E-04	2.51E-01	2.35E-01
9	1.68E+00	5.63E+00	6.56E-04	2.08E-01	1.39E-01
10	1.64E+00	5.06E+00	4.69E-04	1.72E-01	7.60E-02
11	1.60E+00	4.59E+00	3.32E-04	1.44E-01	3.55E-02
12	1.54E+00	4.21E+00	2.33E-04	1.26E-01	1.46E-02

Table S5. Cole-Cole fit values for **2**.

T (K)	ChiS	ChiT	Tau	Alpha	Residual
1.8	7.63E-01	1.03E+01	2.08E-02	1.87E-01	2.48E-01
2.2	5.61E-01	8.18E+00	4.44E-03	1.27E-01	4.77E-01
2.6	4.60E-01	6.98E+00	1.48E-03	8.62E-02	2.99E-01
3.0	3.85E-01	6.13E+00	6.55E-04	6.72E-02	1.85E-01
3.4	3.26E-01	5.44E+00	3.44E-04	5.47E-02	1.55E-01
3.8	2.44E-01	4.91E+00	2.03E-04	5.44E-02	6.35E-02
4.2	1.09E-01	4.46E+00	1.28E-04	5.72E-02	6.43E-02
4.6	3.70E-14	4.07E+00	8.51E-05	5.44E-02	6.61E-02
5.0	7.72E-14	3.76E+00	6.11E-05	5.01E-02	6.64E-02

Theoretical calculations

Table S6. RASSI energies of the lowest spin-orbit states (cm^{-1}) on Dy^{III} ions in **1**-**3**.

Complex **1**		Complex **2**	Complex **3**
Dy1	Dy2		
0.000	0.000	0.000	0.000
53.345	24.445	18.565	59.493
59.010	56.035	48.788	79.398
174.916	121.730	119.846	166.121
301.102	226.448	224.740	287.908
390.480	271.916	244.469	354.180
526.076	284.097	283.063	495.316
614.436	348.113	404.323	583.796
3090.442	3059.765	3051.985	3082.352
3111.166	3081.134	3075.694	3108.688
3147.580	3106.949	3090.948	3145.195
3269.323	3148.513	3139.467	3256.815
3304.638	3160.972	3158.694	3293.832
3349.834	3181.686	3191.939	3331.414
3381.385	3208.322	3247.045	3357.438
5646.362	5651.807	5642.153	5637.544
5750.471	5675.291	5659.300	5734.113
5779.300	5693.389	5681.521	5763.071
5841.655	5713.702	5711.434	5831.963
5869.394	5732.092	5764.310	5866.117
5931.062	5766.185	5778.617	5918.384
7822.222	7824.449	7817.546	7814.740
7916.119	7841.687	7823.823	7892.631

7980.824	7871.796	7867.892	7977.705
8025.166	7900.746	7925.255	8022.696
8103.793	7952.397	7958.431	8086.862
9566.373	9526.765	9525.407	9553.752
9613.001	9537.510	9534.960	9593.929
9616.185	9557.490	9554.239	9605.033
9632.661	9585.832	9572.138	9623.949
9694.935	9600.261	9591.802	9677.616
9729.648	9627.501	9630.011	9713.497
9799.470	9652.672	9653.130	9791.263
9805.089	9668.433	9675.221	9801.492
9842.414	9687.695	9705.995	9838.003
9971.643	9764.619	9770.874	9942.120
11016.657	10988.609	10985.424	11015.357
11103.754	11019.770	11002.062	11095.229
11306.483	11133.678	11156.770	11279.115
11823.505	11734.595	11728.022	11806.326
11871.986	11759.498	11763.718	11858.436
11917.666	11775.796	11777.941	11897.976
11939.430	11797.077	11800.125	11925.620
11975.383	11824.857	11826.604	11960.428
13549.159	13472.290	13470.500	13536.565
13684.464	13564.416	13561.679	13666.761
13706.454	13576.735	13580.981	13691.359
13752.072	13603.808	13605.806	13734.996
14978.842	14888.410	14887.241	14968.268
15065.215	14954.158	14954.769	15048.397
15104.139	14965.587	14966.577	15086.887
16040.020	15927.687	15925.903	16024.413

16056.781	15932.197	15934.623	16039.588
16637.103	16520.334	16520.878	16621.005
38844.016	38814.936	38783.091	38830.935
38873.145	38843.196	38829.502	38858.630
38936.360	38862.093	38861.501	38918.950
39054.837	38878.517	38891.969	39030.478
40209.600	40200.227	40169.325	40196.068
40351.763	40228.900	40219.039	40331.850
40428.163	40277.456	40303.873	40404.243
41299.418	41217.680	41209.252	41281.229
41346.481	41232.140	41233.960	41325.823

Table S7. SINGLE_ANISO computed crystal field parameters for Dy^{III} ions in compounds **1-3**. B_k^q is the crystal field parameter and O_k^q is the extended Stevens operator. The quantization axis is chosen to be the main magnetic axis of the ground pseudo-Doublet. The major components in the Table are in bold font.

k	q	B_k^q	B_k^q	B_k^q	B_k^q
		Complex **1**		Complex **2**	Complex **3**
		Dy1	Dy2		
2	-2	-0.42	0.60	**1.05**	-0.61
	-1	**2.59**	**0.65**	**-1.25**	**-2.76**
	0	-1.49	-0.28	-0.57	-1.10
	1	**-1.66**	**0.81**	**-0.92**	**-2.81**
	2	0.31	0.12	0.1	0.13
4	-4	-0.03	-0.03	0.01	-0.03
	-3	-0.09	-0.01	0.05	0.04
	-2	0.02	0.003	-0.005	0.02
	-1	-0.06	-0.02	0.04	0.06
	0	0.004	-0.008	-0.003	-0.003
	1	-0.03	-0.005	0.03	0.03
	2	0.02	0.002	0.01	0.03
	3	0.08	0.03	-0.02	-0.06
	4	0.01	-0.03	-0.03	-0.03

References:

1. S. Trofimenko, J. R. Long, T. Nappier and S. G. Shore, in *Inorganic Syntheses*, John Wiley & Sons, Inc., 1970, DOI: 10.1002/9780470132432.ch18, pp. 99-109.
2. Bruker-AXS, *Journal*, 2015.
3. G. M. Sheldrick, *SADABS*, 1996.
4. G. M. Sheldrick, *Acta Crystallogr. Sect. A, Found. and Adv.*, 2015, **71**, 3-8.
5. G. M. Sheldrick, *Acta Crystallogr. Sect. C, Struc. Chem.*, 2015, **C71**, 3-8.
6. O. V. Dolomanov, L. J. Bourhis, R. J. Gildea, J. A. K. Howard and H. Puschmann, *Journal of Applied Crystallography*, 2009, **42**, 339-341.
7. W. Pennington, *Journal of Applied Crystallography*, 1999, **32**, 1028-1029.
8. C. F. Macrae, P. R. Edgington, P. McCabe, E. Pidcock, G. P. Shields, R. Taylor, M. Towler and J. van de Streek, *J. Appl. Crystallogr.*, 2006, **39**, 453-457.